Kinetics of Microbial Sulfate Reduction at Pescadero Marsh Natural Preserve, Pescadero, California

Kyle B. Carbajal

ABSTRACT

Soils act as open biogeochemical reactors where water, air, minerals and organic matter interact with microorganisms to drive the rates of chemical changes. In submerged sediments and soils, dissimilatory sulfate (SO_4^{2-}) reduction is an alternative respiration pathway utilized by microorganisms for growth and metabolism in the absence of oxygen. At Pescadero Marsh Natural Preserve, dissimilatory sulfate reduction in response to the hypoxic/anoxic conditions of the estuary results in seasonal fish kill events of endangered Coho salmon and Steelhead trout. A GIS pilot study of the site revealed that sulfate in the estuary is present in typical concentrations for an estuarine environment. Flow-through reactors and soil slurry incubation experiments determined the rates of sulfate reduction to hydrogen sulfide, which is bound to iron (Fe) as reduced iron sulfides. Sulfate reduction rates determined by soil slurry incubations tend to be an overestimate due to increased microbial accessibility to sedimentary substrates, while flow-through reactors are able to accurately mimic *in situ* rates of sulfate reduction, but are limited by sample isolation. This research suggests that future studies should focus on iron reduction and iron-sulfide re-oxidation to further assess the roles of iron and sulfur cycles at Pescadero Marsh Natural Preserve.

KEYWORDS

Dissimilatory sulfate reduction, ArcGIS, flow-through reactor, soil slurry, HPLC

INTRODUCTION

Chemical reactions in soils are crucial to the stability and health of all ecosystems. Soils act as open biogeochemical reactors where water, air, minerals and organic matter (Brady and Weil 2010) interact with microorganisms to drive the rates of chemical changes (Pallud and Van Cappellen 2006, Laverman et al. 2012). Within submerged sediments and soils the chemical changes that take place determine the crop potential, the distribution of plant and aquatic life, and the capacity for wetlands to act as sinks for terrestrial pollution (Ponnamperuma 1972). With 72% of earth's surface covered by submerged sediments and soils, it is of great ecological importance to understand the biogeochemistry of these sediments (Ponnamperuma 1972). A better understanding of submerged near-shore sediments is critical so that remediation, pollution control, and species preservation strategies may be developed with regard to wetland environments (Lovley 1993).

Estuaries play an integral role in the global economy with 39% of the world's population living within 100km from the coast (Burke et al. 2001). Nearly 95% of the global fishery harvest is caught or reared in coastal waters (Sherman et al. 1993). In the United States, almost three quarters of the economy in generated in coastal states (Colgan 2004). According to 2005 gross state product (GSP) estimates, California is the tenth largest economy in the world, with 86% of California's GSP attributed to coastal counties (Sloan 2006). Furthermore, coastal estuaries slow down and store large volumes of water, preserve human developments, and provide ecological, recreational, and other health benefits (Sloan 2006). By slowing down the flow of water, estuaries allow pollutants to settle into the sediment where they may be taken up by microorganisms and removed from the water column.

In anaerobic wetland environments, oxygen (O_2) deficiencies force microorganisms to utilize alternative respiration pathways. One such alternative anaerobic respiration pathway, dissimilatory sulfate reduction, alters the physic-geochemical properties of the submerged sediments and soils. In dissimilatory anaerobic respiration, microorganisms living in submerged sediments couple the oxidation of organic matter (OM) to methane (CH_4) and carbon dioxide (CO_2) with the reduction of electron acceptors such as nitrate (NO_3^-), iron (Fe^{3+}), and sulfate (SO_4^{2-}) (Lovley 1993, Li et al. 2011). Dissimilatory sulfate reduction is the dominant microbial respiration pathway in wetlands and saltmarshes, as rates of aerobic respiration are limited for

microorganisms who can no longer couple the reduction of O_2 to the oxidation of OM for growth and energy generation, therefore utilizing SO_4^{2-} as the next major terminal electron acceptor (Howes et al. 1984, Kostka et al. 2002). Due to the variety of climates, ecologies, and chemistries observed between wetland environments – even on local scales – remediation strategies must be developed on a case-by-case basis.

Pollution, habitat loss, overexploitation, invasive species and climate change are the greatest threats to the ecological health of estuarine environments (Sloan 2006). Fish kills, natural and anthropogenic, are the most obvious indicators of coastal degradation and are often associated with hypoxic (<2 ppm [DO]) and anoxic (<0.5 ppm [DO]) events as well as anthropogenic nutrient enrichments (Diaz and Rosenberg 1995, Sloan 2006). Fish kill events may be attributed to rapid changes in DO concentrations such as after storms and sandbar breaching events that mix hypoxic bottom-waters with the water column, resulting in anoxia and higher sulfide concentrations (Fallsen et al. 2000, D'Avanzo and Kremer 1994). Sulfate reducing bacteria in anaerobic environments obtain energy for growth and metabolism by oxidizing organic compounds while reducing sulfate (SO_4^{2-}) to hydrogen sulfide (H_2S) in a process known as dissimilatory sulfate reduction (Lovley 1993). H_2S is a toxic, colorless gas, most notable for its foul odor of rotten eggs detectable by humans at concentrations as low as 0.47ppb (Powers-Schilling 1995). In general, at pH < 7, hydrogen sulfide (H_2S) in in the unionized form, whereas at pH > 7, bisulfide (HS^-) is the predominate form. Theede (1969) showed that mortality was 20% when H_2S was added to hypoxia experiments. At the Pescadero Marsh Natural Preserve, it is believed that the mixing and oxidation of FeS compounds in the water increases the biochemical oxygen demand (BOD), acidifying the water, increasing concentrations of unionized H_2S.

The Pescadero Marsh Natural Preserve (PMNP) is a seasonal tidal and intermittent estuary formed at the mouths of Pescadero and Butano creeks, where mass fish kills have been observed every year since 1995; the unpleasant odor of hydrogen sulfide (H_2S) gas has been detected for decades (Bradshaw et al. 2008; Viollis 1979). The estuary is separated from the ocean for long periods of time by a sandbar, which creates anoxic zones in the marsh waters. When the sandbar is breached by heavy rain, storms, or anthropogenic interactions, the ocean and marsh waters begin to mix, and the top oxic layers of the estuary are drained off leaving behind only hypoxic/anoxic waters, and killing many fish (Sloan 2006). It is hypothesized that these fish kill events are associated with rapid changes in dissolved oxygen (DO) concentrations, resulting in hypoxic

([DO] < 2 ppm) and anoxic conditions ([DO] < 0.5 ppm). As DO in the water is depleted, microorganisms rely on the reduction of sedimentary sulfate to accommodate their energy needs, releasing H_2S (g) into anoxic zones of the marsh according to a simplified reaction (Eq. 1) for OM substrates (Lovley 1993, Pallud and Van Cappellen 2006):

$$2CH_2O + SO_4^{2-} \rightarrow 2HCO_3^- + H_2S \quad \text{(Eq. 1)}$$

Bradshaw et al. (2008) have hypothesized that these fish kill events may be due to the oxidation of toxic sulfur compounds (ex. reduced iron sulfides) of the anoxic deep-water zones mixing with incoming salt-water, which alters salinity, pH, and other environmental conditions necessary for the survival of federally protected steelhead trout, Coho salmon, and tidewater goby (Bradshaw et al. 2008). However, adequate remediation strategies to address the toxic waters at Pescadero have yet to be discerned with regard to the effects of microbial respiration via dissimilatory sulfate reduction. A more complete understanding of the biogeochemical processes at PMNP is required before an adequate solution can be proposed to save the fish.

The goal of my research is to assess and understand the biogeochemical characteristics of PMNP, and ultimately to determine the role that dissimilatory sulfate reduction plays in the wetland ecosystem. This study will look at sedimentary samples using ArcGIS software, soil slurry incubations, flow-through reactors, high-pressure liquid chromatography (HPLC), and ion-specific electrodes to determine whether or not the sulfide concentrations are naturally high in the sediment or in the water. I will also try to determine which biogeochemical factors are associated with sulfate concentrations, and how those may influence the rates of sulfate reduction. This research may be used to provide potential restoration methods and prevent future fish kills at PMNP.

METHODS

Site description

Pescadero Marsh Natural Preserve (PMNP) is the largest coastal watershed between San Francisco and Santa Cruz. PMNP is a seasonal tidal and intermittent estuary located just 60 km south of San Francisco, and it is home to many species of wildlife including several species of fish and over 200 species of migratory birds. The marsh preserve is composed of multiple habitats: a tidal estuary, a freshwater marsh, a brackish water marsh, riparian woods, and northern coastal brush. The 243-acre (983 m^2) preserve is the most extensive wetland habitat along the coast of the San Francisco peninsula (Figure 1).

Figure 1. Aerial photography of Pescadero Marsh Natural Preserve, CA (2014). The straight-line distance from the study site to San Francisco (a) is approximately 60 km. The study site (b) is approximately 983 m^2. Map data: ©2014 Google, CSUMB SFML, CA OPC.

Sampling strategy

Sedimentary samples and water samples were collected on November 1, 2013 and December 4, 2013 from locations along the perimeter of the estuary (Figure 2). A Garmin GPSMAP 76CSx handheld GPS unit was used to record the date, time, and geographic coordinates

at each sampling site. 37 sampling locations were chosen, and 7 samples were collected from each location. All samples were collected under water and sealed in airtight containers to preserve anaerobic conditions and prevent re-oxidation. The 7 samples collected at each site were a combination of 2 soil and 5 water samples. The 2 soil samples were soil cores (250 g mason jars filled with soil and compacted by hand) collected from the first 15 cm of sediment. The 5 water samples from each location were collected at approximately 0.5 m depth as follows: 1 L for biochemical oxygen demand (BOD), 1 L for alkalinity (Alk), 0.5 L for total phosphorus (TotP), 0.5 L for dissolved iron (DissFe), and 0.5 L as extra water. Additionally, flow-through reactor (FTR) cores were prepared at 4 sample locations (Appendix A). All samples were stored in a refrigerator at 4 °C before analysis. Water samples for BOD, Alk, TotP, and DissFe were sent to Delta Environmental Labs, LLC in Benicia, CA and analyzed for their respective characteristics.

GIS modeling and correlation/regression pilot study

The sedimentary and water samples taken from PMNP were analyzed in lab for a wide range of chemical characteristics. ArcGIS 10.2 (2014) software was used to spatially plot the data and visually analyze changes in characteristics across the landscape (Appendix A). The GIS was used to try and visually determine which variables may influence sulfate concentrations at PMNP, and also to determine if sulfate concentrations could be estimated in the field using a model based on easily obtainable metrics such as pH or DO.

A correlation/regression was done using the R 3.0.3 statistical software package (R Development Core Team 2014). Two separate correlation matrices were generated using the Pearson product-moment correlation coefficient (PPMCC), one for sulfate in the water compared with other water characteristics, and one for sulfate in the sediment compared with other sedimentary characteristics. Correlation coefficients were classified as: perfect, 1; Strong, 0.7-0.9; and moderate, 0.4-0.6 (Dancey and Reidy 2004). Two linear models for predicting sulfate concentrations were then generated using characteristics that had correlations classified as moderate or greater with either sedimentary sulfate or water sulfate.

Soil slurries

Preparation of solutions

Soil slurries may be used to determine the rates of microbial processes in sediments. However, reaction kinetics in soil slurries often overestimate the rates of reactions when compared to those expected from *in situ* conditions (Laverman et al. 2012). Six soil slurries were prepared in an anaerobic chamber (3% H_2 (g), 97% N_2 (g)) using samples from sampling locations 165, 174, 182, 183, 185, and 187 (Figure 2). To prepare the slurry for a single sampling location, 30 g of soil was added to 1 L of deionized water that had been purged with N_2 (g), and mixed completely. 125 mL of soil slurry was distributed into 6 glass serum bottles. Input solutions with 6 known concentrations of sulfate (1, 2, 4, 6, 8, and 10 mM) were made (Table 1), and 125 mL of each input solution was added to the corresponding serum bottle containing 125 mL of soil slurry. Each serum bottle was then capped with a rubber stopper, and crimped with an aluminum seal. The serum bottles were stored at room temperature on an industrial shaker to prevent the suspended sediment from settling.

Table 1. Constituents of prepared sulfate standard solutions. Six standard solutions were prepared with known [SO_4^{2-}]. [Br^-] and [Cl^-] were held constant across solutions. Constituent concentrations in standards are doubled due to 1:1 dilution used in soil slurry experiments.

Std. Solution	SO_4^{2-}	Br^-	Cl^-	H_2O
1	2 mM Na_2SO_4	4 mM KBr	52.6 mM NaCl	Fill to 1 L
2	4 mM Na_2SO_4	4 mM KBr	52.6 mM NaCl	Fill to 1 L
3	8 mM Na_2SO_4	4 mM KBr	52.6 mM NaCl	Fill to 1 L
4	12 mM Na_2SO_4	4 mM KBr	52.6 mM NaCl	Fill to 1 L
5	16 mM Na_2SO_4	4 mM KBr	52.6 mM NaCl	Fill to 1 L
6	20 mM Na_2SO_4	4 mM KBr	52.6 mM NaCl	Fill to 1 L

Sampling and analysis

Using a syringe, approximately 2 mL of sample was drawn from each serum bottle at 24-hr intervals (t = 0 days through t = 15 days). The drawn samples were filtered with Sartorius Minisart 45 μm syringe filters and transferred into individual 2 mL eppendorf tubes. 0.2 – 0.3 mL were then drawn from each eppendorf tube and analyzed using a Dionex LC20 (HPLC) Chromatography Enclosure, equipped with an AG23 guard column and an AS23 analytical

column. The chromatography enclosure was operated using a Dionex GP40 gradient pump and a Dionex ED40 electrochemical detector; all controlled using PeakNet 5.21 software (Dionex 2001). Each sample run was 20 minutes long with a flow rate of 1 mL/min using an eluent composition of 7.2 mM Na_2CO_3 and 1.28 mM $NaHCO_3$. Three main peaks were determined for each sample, in order of size from smallest to largest molecule (Cl^-, Br^-, SO_4^{2-}), and the area under each peak was recorded using Excel 2011 (Microsoft Corporation 2010).

Flow-through reactors (FTR)

Flow-through reactors preserve the physical integrity of sedimentary samples by mimicking *in situ* conditions, and may be used to accurately measure the redox reaction rates of the samples. The reactor cells were prepared in the field using Plexiglas rings of 1-2 cm length by 4.7 cm inside diameter (Figure 3). To collect each sample, the Plexiglas ring was pressed into the sediment like a cookie cutter and removed with an intact sedimentary soil profile. A 0.2 µm nitrocellulose and a glass fiber filter were used to cover the top and bottom sedimentary surfaces of each cell. Two plastic end caps, held together by screws, enclosed each cell, and O-rings within each cap prevented leakage. Each cap contained a small input/output channel in the center and radial grooves to ensure a homogenous flow of input solution across the sediment slice (Pallud et al. 2007).

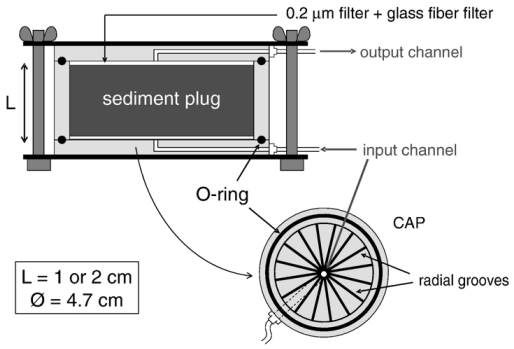

Figure 3. Flow through reactor cell. Side view of a flow-through reactor cell with top view of cap. Figure used with permission (Pallud et al. 2007).

A peristaltic pump was used to continuously supply the sedimentary samples with known concentrations of the reactive solutes (SO_4^{2-}) in deionized water, with bromine (Br^-) as a flow

tracer (Laverman et al. 2006, Pallud et al. 2007). An automated fraction collector was used to regularly collect the outflow solution, and the input solution was purged continuously with Argon (g) to maintain anaerobic conditions. Salinity of the input was adjusted using NaCl to match the salinity measured in the field (Pallud et al. 2007). The flow rate and the composition of the input solution remained constant until the composition of the output fluid no longer changed significantly with time.

Sampling and analysis

Four FTR samples were prepared in the field for sample sites 165, 176, 182, and 185 (Figure 2). The FTR samples were sampled and run through the Dionex LC20 HPLC in identical fashion to the soil slurry samples, with a flow rate of 1 mL/min and an eluent composition of 7.2 mM Na_2CO_3 and 1.28 mM $NaHCO_3$. Each FTR sample was run twice to replicate the results for each sample.

Determination of sulfate reduction rates (SRR) for SS and FTR experiments

To determine the rates of sulfate reduction for both the soil slurry and flow-through reactor experiments, $[SO_4^{2-}]$ (mM) was first calculated for each eppendorf tube using the area under the sulfate peak as recorded by the chromatography instruments (Eq. 2):

$$\left[{SO_4}^{2-}\right](mM) = \frac{\int {SO_4}^{2-}\ peak}{calibration\ number} \cdot molecular\ weight^{-1} \quad \text{(Eq. 2)}$$

Equation 1 can also be applied to Cl^- and Br^- to calculate $[Cl^-]$ or $[Br^-]$ by changing the calibration number and the molecular weight. The calibration number is a variable established when calibrating the Dionex LC20 instrument, which establishes the sensitivity of the instrument's detection capability for each molecule and allows one to convert from the detected units of Sieverts to a molar concentration.

The outflow concentration for each sample was then calculated as the average sulfate concentration for the sample across all time points (Eq. 3):

$$\left[SO_4{}^{2-}\right]_{out}\,(mM) = \frac{\left(\left[SO_4{}^{2-}\right]_1 + \left[SO_4{}^{2-}\right]_2 + \ldots + \left[SO_4{}^{2-}\right]_n\right)}{n} \quad \text{(Eq. 3)}$$

The steady-state sulfate concentration for each serum bottle was then calculated as the average between the standard input solution and its respective output (Eq. 4).

$$Steady-state\left[SO_4{}^{2-}\right](mM) = \frac{\left(\left[SO_4{}^{2-}\right]_{std.}(mM) + \left[SO_4{}^{2-}\right]_{out}(mM)\right)}{2} \quad \text{(Eq. 4)}$$

The steady-state sulfate concentration was used as the baseline for the sample and compared to the outflow concentrations. Sulfate reduction rates (SRR) were then calculated for all samples as the difference between input and outflow sulfate concentrations, divided by the sample time, and corrected for proper units (Eq. 5).

$$SRR\,(nmol\cdot cm^{-3}\cdot h^{-1}) = \frac{\left(\left[SO_4{}^{2-}\right]_{std.}(mM) - \left[SO_4{}^{2-}\right]_{out}(mM)\right)}{time\,(h)\cdot slurry\ concenentration\left(\frac{g}{L}\right)}\cdot wet\ density\left(\frac{g}{cm^3}\right)\cdot 10^6 \quad \text{(Eq. 5)}$$

SRR was graphed as a function of steady state concentration and plotted against Hanes-Woolf and Lineweaver-Burk transformations of Michaelis-Menten kinetic parameters to determine the maximum rates of sulfate reduction for all samples.

RESULTS

GIS and correlation/regression analysis

Upon visual inspection of each map, some characteristics such as nitrogen, organic carbon, C:N, salinity, sulfate, and pH show changes or concentration gradients across the landscape. Characteristics that do not show significant changes across the landscape include: alkalinity, iron concentrations (Fe(II), Fe(III), dissolved Fe), and total phosphorus concentrations. The GIS proved to be an interesting tool for viewing individual characteristics across the landscape, but not useful for determining relationships between multiple variables.

The correlation matrices did derive some relationships between water/sedimentary sulfate and their respective characteristics. Sulfate in the water, dissolved iron, salinity, and water pH were all moderately correlated (Appendix B1). A linear model was generated to describe the relationship between sulfate in the water and these characteristics (Table 2).

Table 2: Linear model for prediction of [SO_4^{2-}] in water.

	Estimate	Std. Error	t value	Pr(>|t|)
Intercept	-2.0448	1.4593	-1.401	0.170838
DissFe (ppm)	-1.2344	0.33175	-3.721	0.000762
Salinity (%)	0.27772	0.07167	3.875	0.000497
Water pH	0.34161	0.19026	1.795	0.082025

$R^2 = 0.66$ F = 20.87 on 3 and 32 DF p = 1.118e-07

Sulfate (mM) = -2.0448 - 1.2344·DissFe(ppm) + 0.27772·Salinity(%) + 0.34161·Water pH

Sedimentary sulfate was found to have a moderate correlation with soil pH and total sulfide (Appendix B2). A linear model was also created to describe sedimentary sulfate in terms of the correlated characteristics (Table 3).

Table 3: Linear model for prediction of [SO_4^{2-}] in sediment.

	Estimate	Std. Error	t value	Pr(>|t|)
Intercept	344.1478	211.6368	1.626	0.120
Total Sulfide	-0.1540	0.4819	-0.319	0.753
Soil pH	-37.0673	32.2705	-1.149	0.265

$R^2 = 0.069$ F = 7.06 on 2 and 19 DF p = 0.5063

Sulfate (mg/kg) = 344.1478 – 37.0673·Soil pH – 0.1540·Total S^{2-} (mg/kg)

Soil slurry sulfate reduction rates

Sulfate reduction rates (SRR) were calculated as the difference between steady-state input and output SO_4^{2-} concentrations over time for all samples. SRR for the six sample sites used in the soil slurry incubations ranged an order of magnitude, from 80 $nmolcm^{-3}hr^{-1}$for sample 185, to nearly 800 $nmolcm^{-3}hr^{-1}$ for sample 183 (Table 4).

Table 4: SSR and Km for soil slurry incubations.

Site	SRR_{max} (nmol cm^{-3} h^{-1})	K_m (mM)
165	476.20	8.95
174	303.03	5.40
182	476.20	12.33
183	769.23	5.46
185	80.00	1.86
187	588.24	8.59

When plotted as SRR vs. steady-state $[SO_4^{2-}]$, the relationship follows the Michaelis-Menten model for enzyme rate kinetics (Figure 4). SRR increases as the concentration of SO_4^{2-} increases, asymptotically approaching SRR_{max}, the highest reduction rate achieved by the system. K_m represents the reciprocal affinity that sulfate-reducing bacteria have for the sulfate, with lower a K_m indicative of higher affinity.

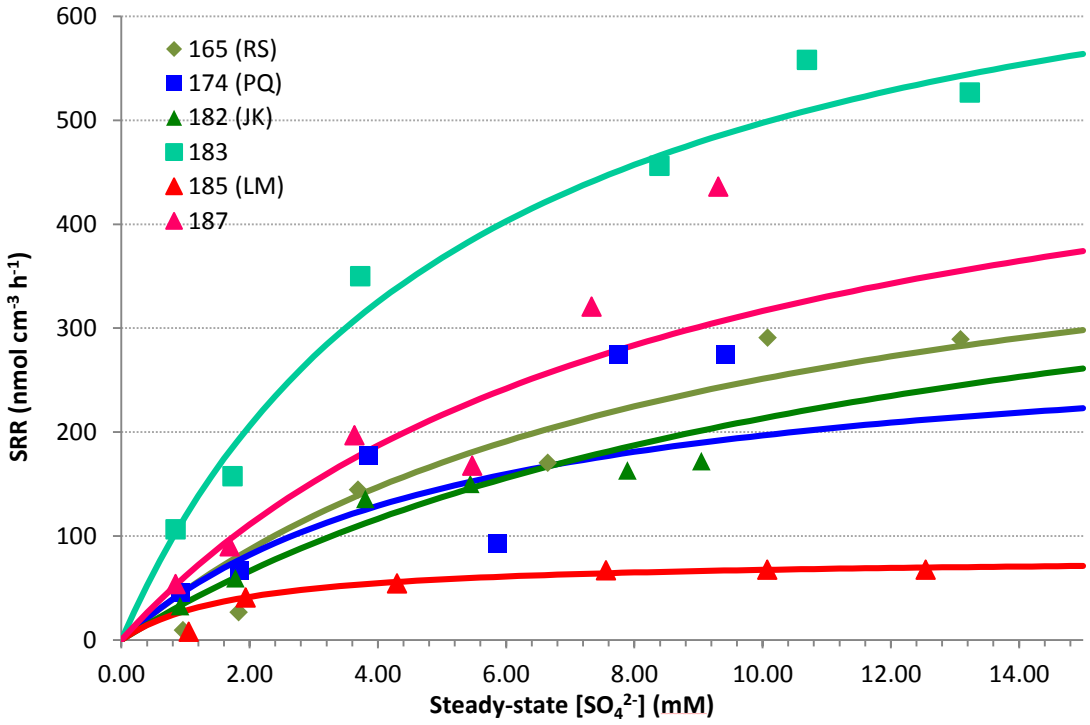

Figure 4. Sulfate reduction rates vs. steady-state [SO_4^{2-}] for soil slurry experiments. Letters in parenthesis indicate the replicated samples used in the flow-through reactor experiments.

Flow-through reactor sulfate reduction rates

Flow through reactor (FTR) experiments were performed on samples 165, 174, 182, and 185. The experiment was duplicated for all samples, and SRR was calculated in the same manner as in the soil slurry experiments. SRR for the FTR experiments were drastically lower than the SRR achieved by the soil slurry experiments for all samples (Table 5).

Table 5: SSR and K_m for flow-through reactors. Average SRR was calculated for the FTR experiments because each sample was duplicated in the FTR experiments. Average SRR is the average of the SRR achieved by each sample in a pair (C. Richards, *unpublished data)*.

Site	Average SRR_{max} (nmol cm^{-3} h^{-1})	Average K_m (mM)
165	94.10	1.05
176	137.6	1.59
182	23.20	0.40
185	62.40	0.60

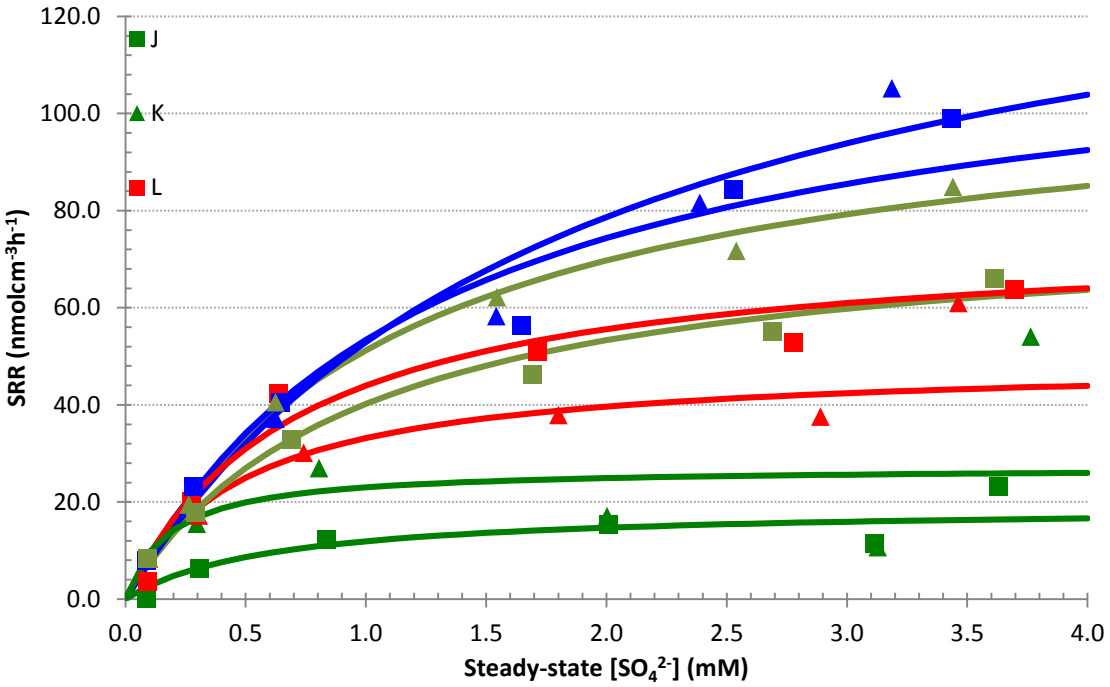

Figure 5. Sulfate reduction rates vs. steady-state [SO_4^{2-}] for flow-through reactor experiments.

DISCUSSION

Coastal estuaries play important roles for both regional and global economies, especially in California, where more than 80% of GSP can be attributed to coastal communities in the forms of fish harvests, recreation, water storage, and other ecological health benefits (Sloan 2006). Fish kills, both natural and anthropogenic, are typically one of the first indicators that an estuarine environment is unhealthy. At the Pescadero Marsh Natural Preserve, the odor of hydrogen sulfide gas has been present for almost half a century (Viollis 1979), yet mass fish kill events have only been reported since the mid 1990s. It has been hypothesized that these fish kill events are due mainly to hypoxia, suffocating the fish (Bradshaw et al. 2008). In order to explain these fish kill events, it is necessary to understand the physic-biogeochemistry of the study site by constructing a water quality model that can explain the major chemical and biological pathways occurring at the study site (C. Richards, *unpublished data*). This, and subsequent studies of PMNP, have

elucidated the significance of sulfur (SO_4^{2-}, HS^-, H_2S), iron (Fe^{2+} and Fe^{3+}), pH, salinity, and dissolved oxygen in the sediment and in the water of PMNP, thus they are all to be included in a future publication assessing the major biogeochemical pathways of the study site (C. Richards, *unpublished data*). Using GIS, soil slurries, and flow-through reactors, I was able to address a small piece of the overall water quality model by measuring the rate of SO_4^{2-} reduction to H_2S. The GIS study concluded that the necessary factors have already been accounted for in the proposed water quality model (C. Richards, *unpublished data*), while the soil slurry and flow-through reactors were able to address the rates of sulfate reduction at the estuary in both closed and open states.

GIS pilot study

A GIS was created as a means for the visualization of a broad range of chemical characteristics in the waters at PMNP prior to sedimentary sulfate analysis. In the initial pilot study only a small subset of data (25 sample points, 11 characteristics) was used to create a model that could be used to predict sulfate concentrations in the water at PMNP. The focus of this model was for predicting sulfate concentrations based upon easier to measure variables, such as water pH, DO concentrations, salinity, etc. The pilot study did result in what appeared to be a successful model for sulfate prediction. However, when applying the same statistical methods to the full data set (37 sample points, 22 characteristics), it became apparent that there is no statistically significant way to predict sulfate based upon only a few easily measured characteristics. An accurate approximation of H_2S, HS^-, and SO_4^{2-} concentrations in water should be determined using more conventional methods, such as mass balance and electroneutrality considerations (Benjamin 2002).

Soil slurry and flow-through reactor experiments

Soil slurry incubation experiments were performed on six samples, selected to match and compare with the FTR experiments. In all cases, SRR determined by the soil slurries were larger than SRR determined by FTR experiments. The large differences in reaction kinetics between the soil slurry and FTR experiments can be attributed to the homogenization and dilution of the sediments in the soil slurry experiments, which disrupts the physical, chemical and microbiological

structure of each sample (Laverman et al. 2006). Furthermore, the deviations from *in situ* conditions (i.e. mixing, dilution) in soil slurry experiments allow for increased microbial access to organic matter, increasing the sediment surface area to volume ratio, which allows for increased substrate utilization by microorganisms, and therefore increased rates of sulfate reduction (Laverman et al. 2006).

With such a large difference in results between soil slurry and FTR experiments it is important to note that each experiment is representative of different conditions at PMNP. When the sandbar is in place (closed state), the waters are typically stratified into an oxic epilimnion, a hypoxic metalimnion, and an anoxic hypolimnion. There is little to no mixing along with little to no suspended sediment in the water column during the closed state, which can last for 8-10 months of the year (C. Richards, *unpublished data*). Therefore, it is feasible to study sedimentary samples during the closed state using flow-through reactors, which mimic *in situ* conditions, and can measure sulfate reduction rates as would be expected in the undisturbed sediment.

However, in the interest of understanding the annual fish kill events at PMNP, it is also important to study the physic-biogeochemical properties of the estuary when the sandbar is breached (open state), because that is historically when the mass fish kill events have been observed. As the sandbar breaches (transition from closed to open state), the oxic epilimnion is drained from the estuary, leaving the hypoxic and anoxic layers, which suggests that microbial sulfate reduction may persist throughout the year. In order to study the open state conditions of the estuary, soil slurries are able to initiate the mixing and turbidity that would be expected during the transition from closed to open state. The kinetics obtained from soil slurry incubations may be more indicative of this transition than the flow-through reactor experiments would elucidate.

Limitations

My original study design consisted of 25 individual sampling locations, and intended to give a good, yet incomplete representation of the conditions at PMNP. However, due to time limitations and instrument failures in the lab, only 6 samples were used in the soil slurry and 4 samples were used in the FTR experiments, which gives a less complete representation of sulfate reduction at PMNP than was initially intended. Further, sampling was not feasible in locations where water depth exceeded roughly 1.5 ft., therefore the samples used in this study are only

representative of the littoral sediments of shores at PMNP. All samples for the FTR and soil slurry experiments were run using an outdated ion chromatography enclosure, which may be less sensitive than necessary to detect any significant reduction in sulfate concentrations. For the soil slurry experiments, the sample solution were intended to be shaken non-stop in between sample points to ensure adequate mixing (Pallud and Van Cappellen 2006), however, after 3 broken shakers it was decided amongst the lab that a lack of shaking would have negligible effects on observed sulfate reduction rates.

Future directions/broader implications

Due to the pH-dependent chemistry of hydrogen sulfide, acidification leads to H_2S as the dominant form, while hydrolysis leads to HS^-. H_2S can vaporize from the water/sediment into the atmosphere, while HS^- precipitates with reduced Fe(II) minerals forming iron sulfides (FeS, FeS_2). Oxidation of the iron sulfides during the marsh's transition to open state decreases DO is water column, and microorganisms are forced to switch from aerobic to anaerobic metabolism. This coincides with an increases is sulfate reduction, iron reduction, precipitation of iron sulfides, and the annual fish kills observed when the sandbar is breached. Future studies at Pescadero should focus on iron reduction and iron sulfide precipitation events to further understand the biogeochemical processes occurring at PMNP (C. Richards, *unpublished data*).

ACKNOWLEDGEMENTS

Thank you Céline Pallud for allowing me to work freely in your lab, use your supplies and equipment, and for sparking my interest in soil chemistry through your ESPM 120 class. Thank you Chandra Richards for allowing me to step in and work on a part of your Ph.D. research, for teaching me proper methods for instrument use and experimentation, and for showing me the utmost patience and kindness in all aspects of this project. Thank you also for the time and effort you put into reading and helping me to revise the many drafts of this thesis. Thank you Eric Huber, Frank Hubinsky, Sarick Matzen, and Clifford Wang for helping out with sample collection and preparation at the field site. Thank you James Hake, Hoai Ngo, Vu Ngo, and Tegan Duong for your help in analyzing the samples and collecting the data used in this study. Thank you to the Cal

Bohrs: Kathryn Liu, Danielle Ngo, Becca Samuel, and Jasmine Thai; my thesis work group, for all of their wonderful comments and help with brainstorming and editing the many drafts of my thesis. Thank you John Battles, Maya Hayden for getting me started on this project in ESPM 100ES and teaching me how to write a successful research proposal. Thank you Anne Murray and Patina Mendez for helping me structure, write, and format a substantive senior thesis in ESPM 175.

REFERENCES

Benjamin, M. M. 2002. Water Chemistry. Waveland Press, Long Grove, Illinois.

Bradshaw, S., C. M. Allen, S. L. Leroy, K. L. Faul, and L. K. Rademacher. 2008. Biogeochemical causes of fish kill events in Pescadero Marsh; San Mateo County, California. Thesis, University of the Pacific, Stockton, California, USA.

Brady, N. C., and R. R. Weil. 2010. Elements of the nature and properties of soils, 3rd edition. Prentice Hall, Upper Saddle River, New Jersey.

Burke, L., Y. Kura, K. Kassem, C. Revenga, M. Spalding, D. McAllister. 2001. Coastal ecosystems, Pilot analysis of global ecosystems. World Resources Institute, Washington, DC.

Cicerone R. J. and R. S. Oremland. 1988. Biogeochemical aspects of atmospheric methane. Global Biogeochemical Cycles 2:299-327.

Colgan, C. S. 2004. The changing ocean and coastal economy of the United States: A briefing paper for governors. National Governors Association.

D'Avanzo, C. and J. N. Kremer. 1994. Diel oxygen dynamics and anoxic events in an eutrophic estuary of Waquoit Bay, Massachusetts. Estuaries 17:131-139.

Dancey, C. and J. Reidy. 2004. Statistics without Maths for Psychology: using SPSS for Windows. Prentice Hall, London.

Diaz, R. J. and R. Rosenberg. 1995. Marine benthic hypoxia: a review of its ecological effects and the behavioral responses of benthic macrofauna. Oceanography Marine Biology Annual Review 33:245-303.

Esri. 2014. ArcGIS version 10.2. Esri, Redlands, California, USA.

Fallsen, G., F. Andersen and B. Larsen. 2000. Life, death and revival of the hypereutrophic Mariager Fjord, Denmark. Journal of Marine Systems 25:313-321.

Howes, B. L., J. W. H. Dacey, and G. M. King. 1984. Carbon flow through oxygen and sulphate reduction pathways in salt marsh sediments. Limnology and Oceanography 29:1037-1051.

Kostka, J. E., A. Roychoudhury, and P. Van Cappellen. 2002. Rates and controls of anaerobic microbial respiration across spatial and temporal gradients in saltmarsh sediments. Biogeochemistry 60:49-76.

Laverman, A. M., P. Van Cappellen, D. van Rotterdam-Los, C. Pallud, and J. Abbell. 2006. Potential rates and pathways of microbial nitrate reduction in coastal sediments. FEMS Microbial Ecology 58:179-192.

Laverman, A. M., C. Pallud, J. Abell, and P. Van Cappellen. 2012. Comparative survey of potential nitrate and sulfate reduction rates in aquatic sediments. Geochimica et Cosmochimica Acta 77:474-488.

Li, Y., S. Y. Park, and J. Zhu. 2011. Solid-state digestion for methane production from organic waste. Renewable and Sustainable Energy Reviews 15:821-826.

Lovley, D. R. 1993. Anaerobes into heavy metal: Dissimilatory metal reduction in anoxic environments. Trends in Ecology and Evolution 8:213-217.

Pallud, C., and P. Van Cappellen. 2006. Kinetics of microbial sulfate reduction in estuarine sediments. Geochimica et Cosmochimica Acta 70:1148-1162.

Pallud, C., C. Meile, A. M. Laverman, J. Abell, and P. Van Cappellen. 2007. The use of flow-through sediment reactors in biogeochemical kinetics: Methodology and examples of applications. Marine Chemistry 106:256-271.

Ponnamperuma, F. N. 1972. The chemistry of submerged soils. Advances in Agronomy 24:29-96.

Powers-Schilling, W. J. 1995. Olfaction: chemical and psychological considerations. Procession of Nuisance Concerns in Animal Management: Odor and Flies Conference, Gainesville, Florida.

R Development Core Team. 2014. R version 3.0.3. R Project for Statistical Computing, Vienna, Austria. www.r-project.org

Sherman, K., L. Alexander and B. Gold. 1993. Large marine ecosystems: Stress, mitigation and sustainability as global units for marine resource management – An ecological perspective. Large Marine Ecosystems: Stress, mitigation and sustainability. AAAS Press, Washington, DC.

Sloan, R. M. 2006. Ecological investigations of a fish kill in Pescadero Lagoon, California. Thesis. San Jose State University, San Jose, California, USA.

Theede, H., A. Ponat, K. Kiroki and C. Schliper. 1969. Studies on the resistance of marine bottom invertebrates to oxygen-deficiency and hydrogen sulfide. Marine Biology 2:325-337.

Thermo Scientific Dionex. 2001. Peaknet version 5.21. Thermo Fisher Scientific, Waltham, Massachusetts, USA.

Viollis, F. S. 1979. The evolution of Pescadero Marsh. Thesis. San Francisco State University, San Francisco, California, USA.

APPENDIX CONTENTS

A. GIS Maps and Figures

B. Correlation Matrices

C. Sulfate Reduction in Soil Slurry Incubations

APPENDIX A: GIS Maps and Figures

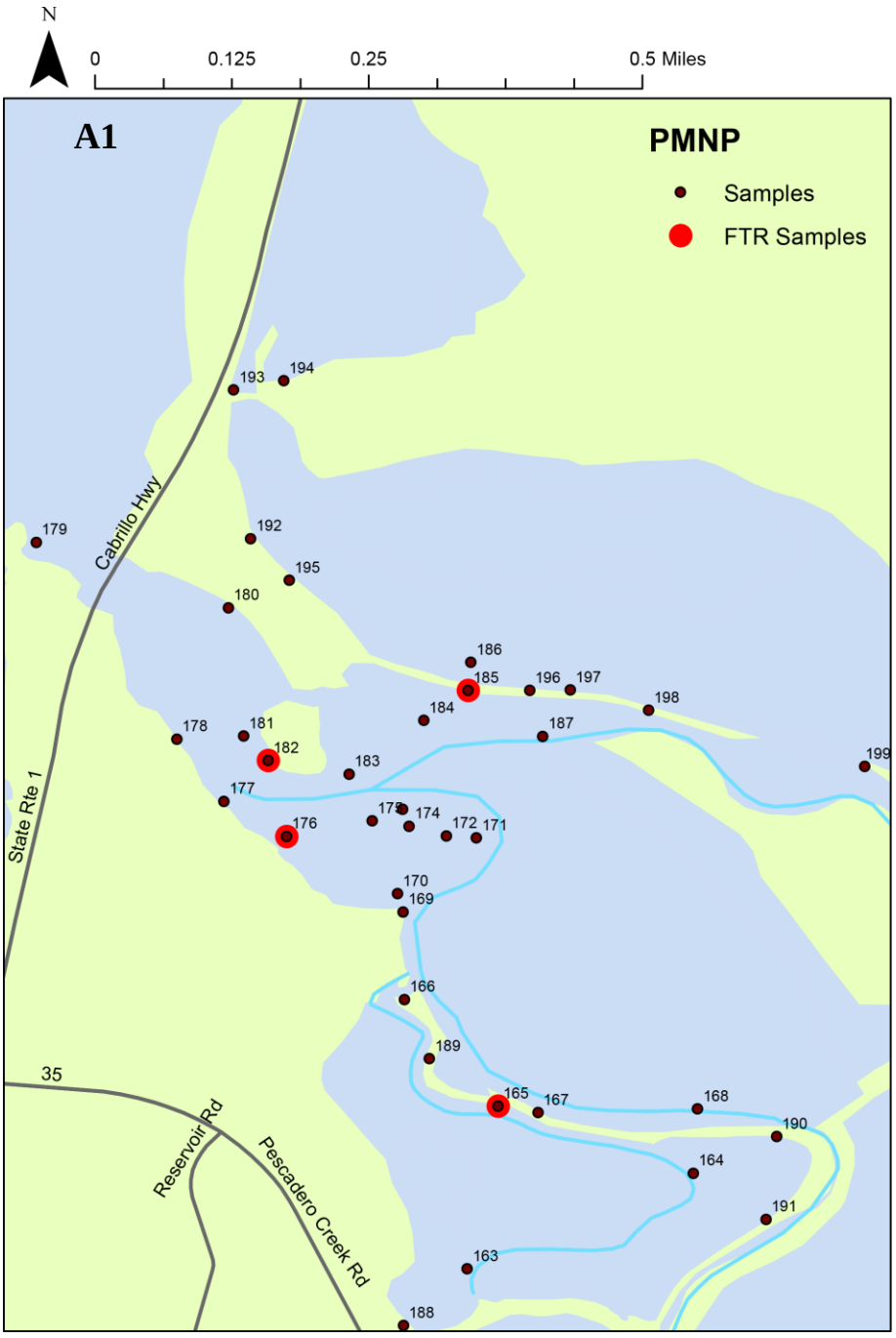

Figure A1. Sampling locations at Pescadero Marsh Natural Preserve. Samples 163 – 187 were collected on November 1, 2013. Samples 188 – 199 were collected on December 4, 2013. Sandbar not pictured between ocean and estuary. Map data: National Hydrography Dataset (NHD) and National Map Viewer (NMV) ©2013 USGS. *Note: the following images (A2-A21) represent the same sample points, but display the various characteristics measured at each sample point.

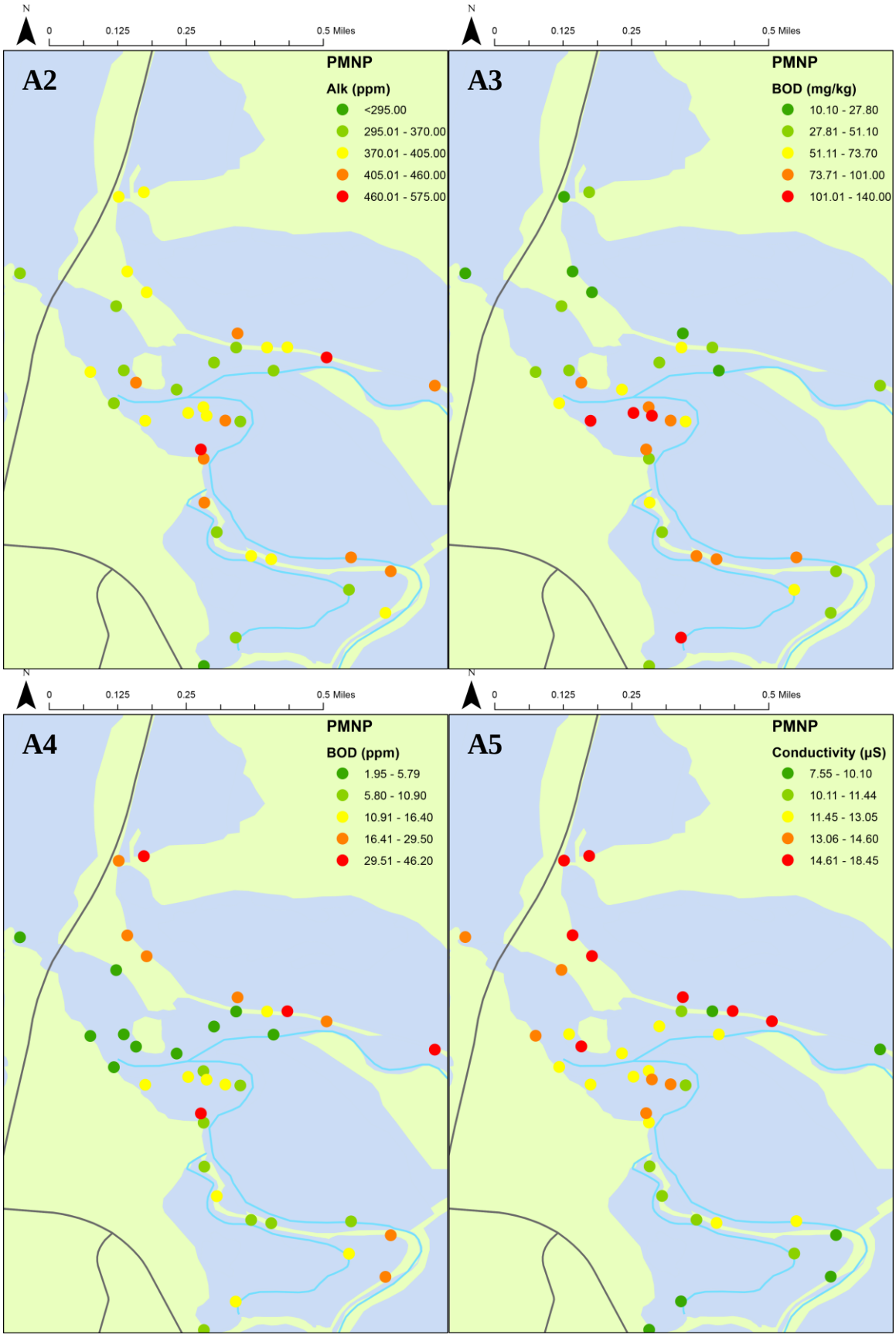
A2
N
0 0.125 0.25 0.5 Miles
PMNP
Alk (ppm)
<295.00
295.01 - 370.00
370.01 - 405.00
405.01 - 460.00
460.01 - 575.00
A3
N
0 0.125 0.25 0.5 Miles
PMNP
BOD (mg/kg)
10.10 - 27.80
27.81 - 51.10
51.11 - 73.70
73.71 - 101.00
101.01 - 140.00
A4
N
0 0.125 0.25 0.5 Miles
PMNP
BOD (ppm)
1.95 - 5.79
5.80 - 10.90
10.91 - 16.40
16.41 - 29.50
29.51 - 46.20
A5
N
0 0.125 0.25 0.5 Miles
PMNP
Conductivity (µS)
7.55 - 10.10
10.11 - 11.44
11.45 - 13.05
13.06 - 14.60
14.61 - 18.45

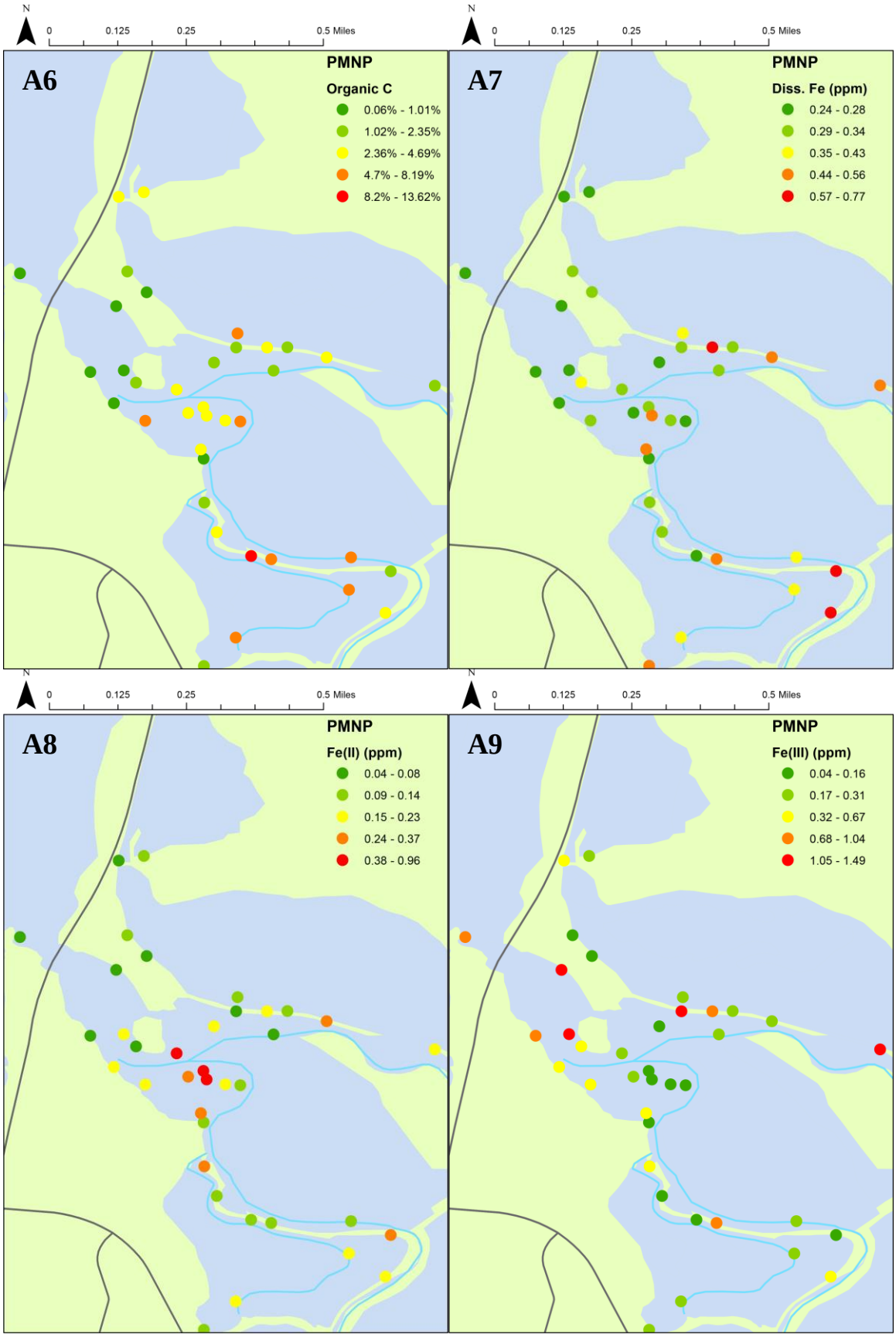
A6
N
0
0.125
0.25
0.5 Miles
PMNP
Organic C
0.06% - 1.01%
1.02% - 2.35%
2.36% - 4.69%
4.7% - 8.19%
8.2% - 13.62%
A7
N
0
0.125
0.25
0.5 Miles
PMNP
Diss. Fe (ppm)
0.24 - 0.28
0.29 - 0.34
0.35 - 0.43
0.44 - 0.56
0.57 - 0.77
A8
N
0
0.125
0.25
0.5 Miles
PMNP
Fe(II) (ppm)
0.04 - 0.08
0.09 - 0.14
0.15 - 0.23
0.24 - 0.37
0.38 - 0.96
A9
N
0
0.125
0.25
0.5 Miles
PMNP
Fe(III) (ppm)
0.04 - 0.16
0.17 - 0.31
0.32 - 0.67
0.68 - 1.04
1.05 - 1.49

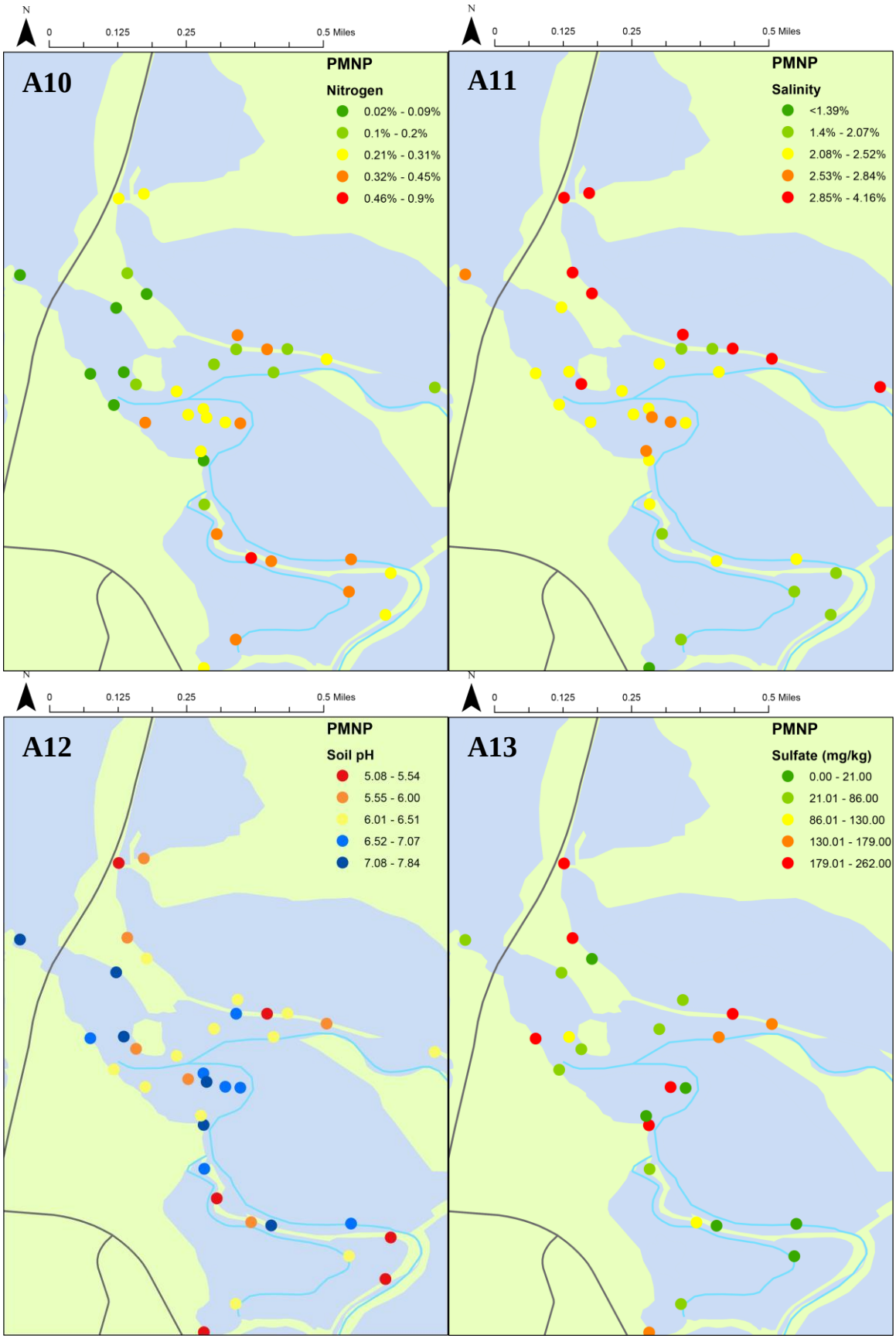
A10
N
0
0.125
0.25
0.5 Miles
PMNP
Nitrogen
0.02% - 0.09%
0.1% - 0.2%
0.21% - 0.31%
0.32% - 0.45%
0.46% - 0.9%
A11
PMNP
Salinity
<1.39%
1.4% - 2.07%
2.08% - 2.52%
2.53% - 2.84%
2.85% - 4.16%
A12
PMNP
Soil pH
5.08 - 5.54
5.55 - 6.00
6.01 - 6.51
6.52 - 7.07
7.08 - 7.84
A13
PMNP
Sulfate (mg/kg)
0.00 - 21.00
21.01 - 86.00
86.01 - 130.00
130.01 - 179.00
179.01 - 262.00

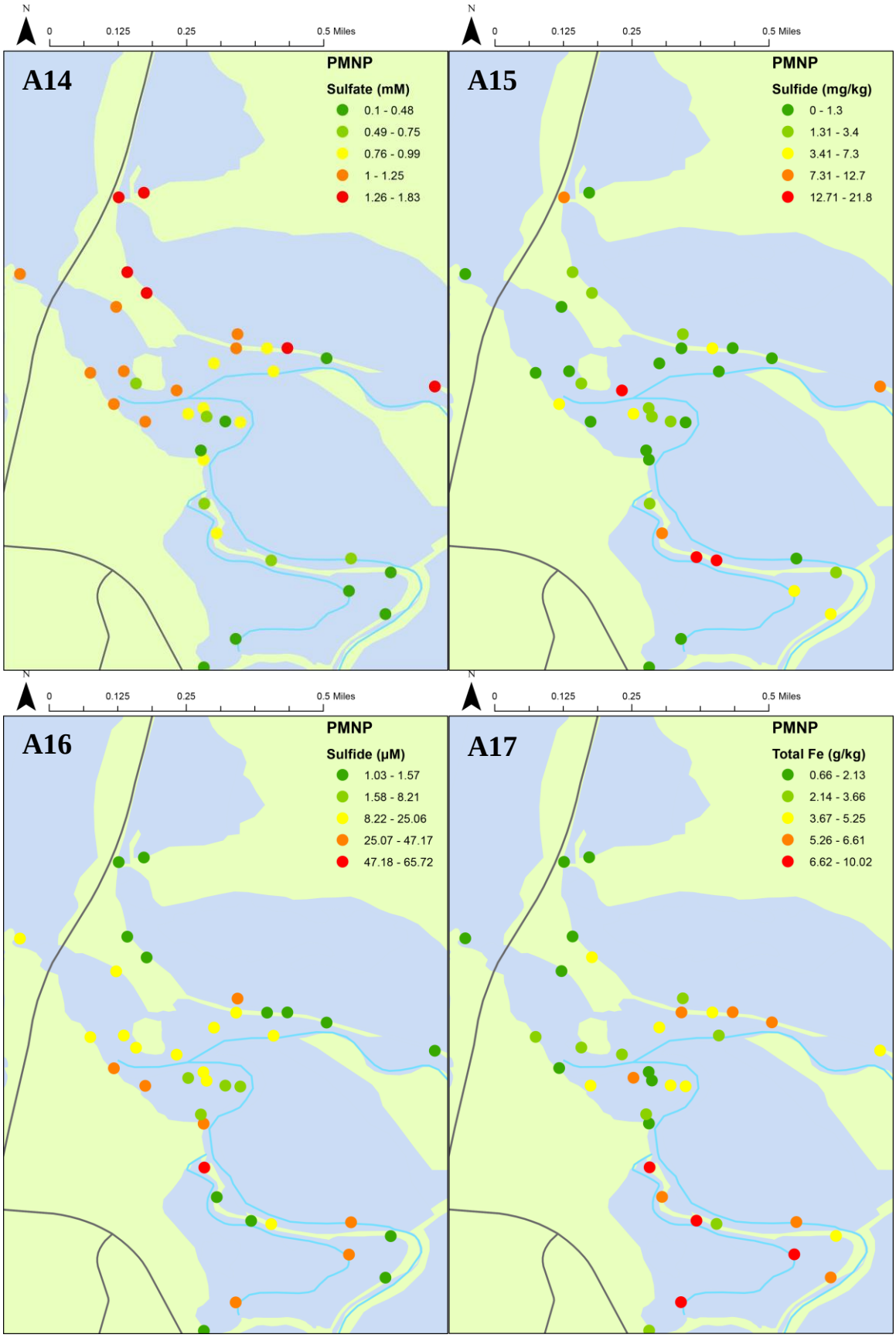
N
0
0.125
0.25
0.5 Miles
A14
PMNP
Sulfate (mM)
0.1 - 0.48
0.49 - 0.75
0.76 - 0.99
1 - 1.25
1.26 - 1.83
A15
PMNP
Sulfide (mg/kg)
0 - 1.3
1.31 - 3.4
3.41 - 7.3
7.31 - 12.7
12.71 - 21.8
A16
PMNP
Sulfide (µM)
1.03 - 1.57
1.58 - 8.21
8.22 - 25.06
25.07 - 47.17
47.18 - 65.72
A17
PMNP
Total Fe (g/kg)
0.66 - 2.13
2.14 - 3.66
3.67 - 5.25
5.26 - 6.61
6.62 - 10.02

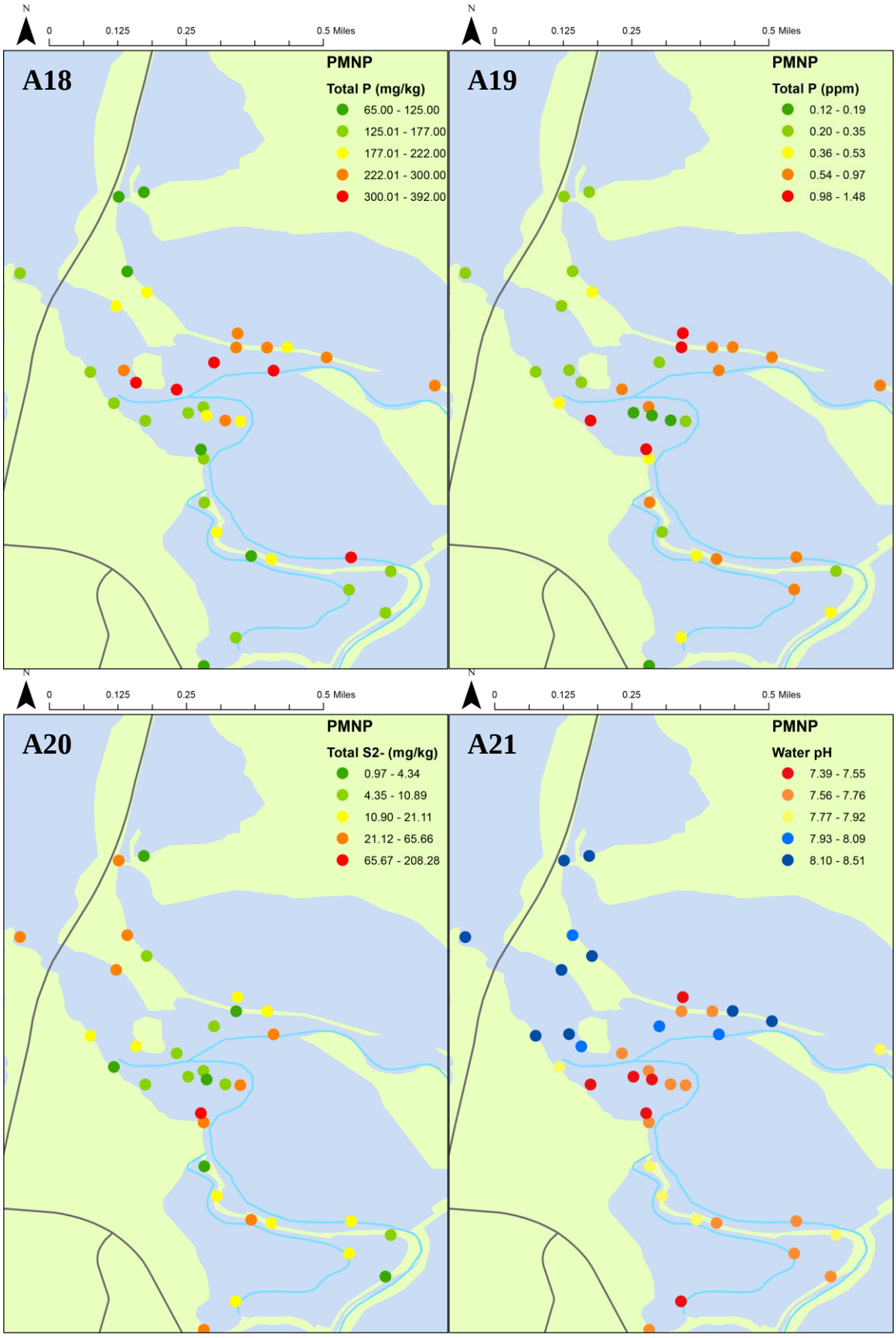
N
0
0.125
0.25
0.5 Miles
A18
PMNP
Total P (mg/kg)
65.00 - 125.00
125.01 - 177.00
177.01 - 222.00
222.01 - 300.00
300.01 - 392.00
A19
PMNP
Total P (ppm)
0.12 - 0.19
0.20 - 0.35
0.36 - 0.53
0.54 - 0.97
0.98 - 1.48
A20
PMNP
Total S2- (mg/kg)
0.97 - 4.34
4.35 - 10.89
10.90 - 21.11
21.12 - 65.66
65.67 - 208.28
A21
PMNP
Water pH
7.39 - 7.55
7.56 - 7.76
7.77 - 7.92
7.93 - 8.09
8.10 - 8.51

APPENDIX B: Correlation Matrices

	Alk (ppm)	BOD (ppm)	Diss. Fe (ppm)	Fe^{2+} (ppm)	Fe^{3+} (ppm)	Salinity (%)	SO_4^{2-} (mM)	S^{2-} (μM)	Tot. P (ppm)	Water pH
Alk (ppm)		0.51	0.28	0.12	-0.10	0.39	-0.30	-0.01	0.30	-0.16
BOD (ppm)	0.51		0.23	-0.04	-0.19	0.62	0.26	-0.42	0.26	0.13
DissFe (ppm)	0.28	0.23		0.16	0.03	-0.25	-0.59	-0.26	0.09	-0.31
Fe^{2+} (ppm)	0.12	-0.04	0.16		-0.31	-0.16	-0.19	0.02	0.02	-0.38
Fe^{3+} (ppm)	-0.10	-0.19	0.03	-0.31		-0.02	0.14	0.08	0.22	0.26
Salinity (%)	0.39	0.62	-0.25	-0.16	-0.02		0.66	-0.30	0.10	0.48
SO_4^{2-} (mM)	-0.30	0.26	-0.59	-0.19	0.14	0.66		-0.20	0.03	0.56
S^{2-} (μM)	-0.01	-0.42	-0.26	0.02	0.08	-0.30	-0.20		0.28	-0.34
Tot. P (ppm)	0.30	0.26	0.09	0.02	0.22	0.10	0.03	0.28		-0.37
Water pH	-0.16	0.13	-0.31	-0.38	0.26	0.48	0.56	-0.34	-0.37	

Figure B1. Correlation matrix for measured water characteristics across all sampled locations. The column and row of interest (sulfate) are colored in light gray. Fields with a correlation coefficient of moderate or greater (> ± 0.4) are colored in dark gray.

	BOD (mg/kg)	Org. C (%)	C:N	N (%)	S^{2-} (mg/kg)	Soil pH	SO_4^{2-} (mg/kg)	Tot. Fe (g/kg)	Tot. P (mg/kg)	Tot. S^{2-} (mg/kg)
BOD (mg/kg)		0.29	0.43	0.28	0.41	0.49	-0.20	0.31	0.20	-0.03
Org. C (%)	0.29		0.66	1.00	0.74	-0.06	0.05	0.59	-0.30	0.74
C:N	0.43	0.66		0.62	0.61	-0.06	0.34	0.15	-0.16	0.49
N (%)	0.28	1.00	0.62		0.71	-0.02	-0.01	0.61	-0.29	0.70
S^{2-} (mg/kg)	0.41	0.74	0.61	0.71		0.18	0.02	0.27	-0.40	0.58
Soil pH	0.49	-0.06	-0.06	-0.02	0.18		-0.59	0.26	0.11	-0.60
SO_4^{2-} (mg/kg)	-0.20	0.05	0.34	-0.01	0.02	-0.59		-0.30	-0.30	0.48
Tot. Fe (g/kg)	0.31	0.59	0.15	0.61	0.27	0.26	-0.30		-0.24	0.19
Tot. P (mg/kg)	0.20	-0.30	-0.16	-0.29	-0.40	0.11	-0.30	-0.24		-0.37
Tot. S^{2-} (mg/kg)	-0.03	0.74	0.49	0.70	0.58	-0.60	0.48	0.19	-0.37	

Figure B2. Correlation matrix for measured sedimentary characteristics across all sampled locations. The column and row of interest (sulfate) are colored in light gray. Fields with a correlation coefficient of moderate or greater (> ± 0.4) are colored in dark gray.

APPENDIX C: Sulfate Reduction in Soil Slurries

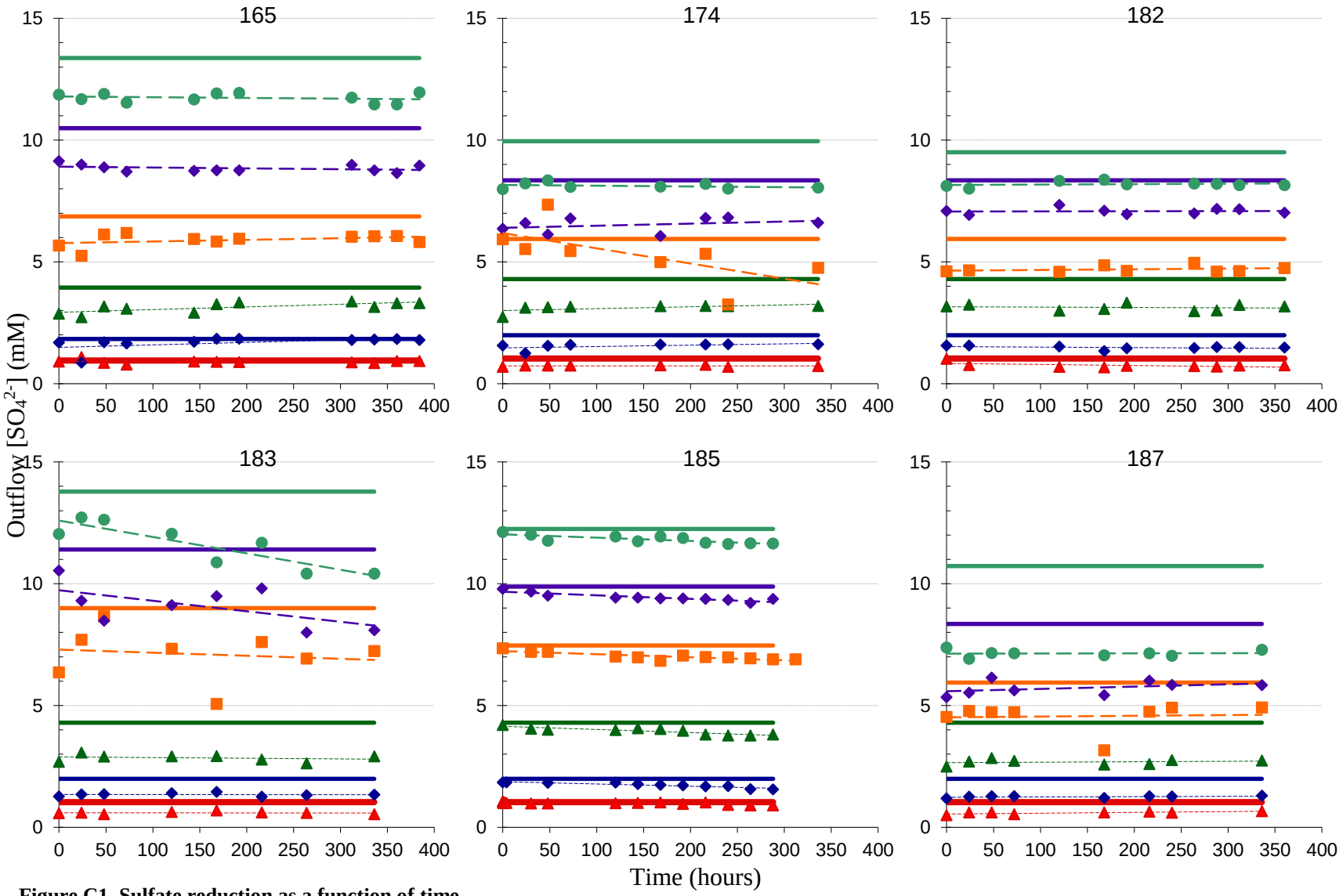

Figure C1. Sulfate reduction as a function of time.